Simulation of the global contrail radiative forcing: A sensitivity analysis

Bingqi Yi,[1] Ping Yang,[1] Kuo-Nan Liou,[2] Patrick Minnis,[3] and Joyce E. Penner[4]

Received 27 September 2012; revised 6 November 2012; accepted 9 November 2012; published 22 December 2012.

[1] The contrail radiative forcing induced by human aviation activity is one of the most uncertain contributions to climate forcing. An accurate estimation of global contrail radiative forcing is imperative, and the modeling approach is an effective and prominent method to investigate the sensitivity of contrail forcing to various potential factors. We use a simple offline model framework that is particularly useful for sensitivity studies. The most-up-to-date Community Atmospheric Model version 5 (CAM5) is employed to simulate the atmosphere and cloud conditions during the year 2006. With updated natural cirrus and additional contrail optical property parameterizations, the RRTMG Model (RRTM-GCM application) is used to simulate the global contrail radiative forcing. Global contrail coverage and optical depth derived from the literature for the year 2002 is used. The 2006 global annual averaged contrail net (shortwave + longwave) radiative forcing is estimated to be 11.3 mW m^{-2}. Regional contrail radiative forcing over dense air traffic areas can be more than ten times stronger than the global average. A series of sensitivity tests are implemented and show that contrail particle effective size, contrail layer height, the model cloud overlap assumption, and contrail optical properties are among the most important factors. The difference between the contrail forcing under all and clear skies is also shown. **Citation:** Yi, B., P. Yang, K.-N. Liou, P. Minnis, and J. E. Penner (2012), Simulation of the global contrail radiative forcing: A sensitivity analysis, *Geophys. Res. Lett.*, *39*, L00F03, doi:10.1029/2012GL054042.

1. Introduction

[2] Contrails are ice clouds produced by aircraft emissions under suitable atmospheric conditions and have optical and radiative properties similar to those of natural cirrus clouds [*Penner et al.*, 1999]. Young contrails are normally line-shaped and short-lived, but can persist for a longer amount of time and grow to transform into old contrail cirrus clouds indistinguishable from natural cirrus [*Minnis et al.*, 1998]. Contrails have drawn considerable attention in research studies on aviation-climate interactions, because contrail forcing has been found to outweigh the impact of direct aircraft CO_2 emissions and is regarded as the most significant effect of aviation on climate [*Burkhardt and Karcher*, 2011; *Sausen et al.*, 2005]. Furthermore, the question arises whether the radiative effect of contrails may be responsible for considerable diurnal temperature variations in some regional areas where air traffic activities are significant [*Hong et al.*, 2008; *Travis et al.*, 2002].

[3] Although contrail detection from satellite observations [*Iwabuchi et al.*, 2012; *Minnis et al.*, 2005] is possible, the direct assessment of contrail radiative forcing from a satellite observational perspective [*Meyer et al.*, 2002] remains a challenge. Under these circumstances, simulations based on numerical models of various complexities ranging from simple offline radiative transfer models to sophisticated online global climate models, have been employed for the estimation of contrail radiative forcing. For example, *Minnis et al.* [1999] used the Fu-Liou radiative transfer model together with prescribed contrail properties (coverage, optical depth, particle size, etc.) and computed the global mean radiative forcing for line-shaped contrails to be as high as 20 mW m^{-2} in 1992 and estimated to be 100 mW m^{-2} in 2050. However, many global climate model studies focus on parameterizing contrail formation, evolution, transformation, and dissipation processes by using aircraft emission inventory data. *Ponater et al.* [2002] developed the first line-shaped contrail parameterization for use in the ECHAM4 general circulation model and found substantially smaller contrail radiative forcing. *Burkhardt and Karcher* [2009] implemented a physical process-based prognostic contrail parameterization scheme and included the consideration of aged contrail cirrus in the GCM. *Rap et al.* [2010a, 2010b] adapted *Ponater et al.*'s [2002] contrail parameterization scheme, applied it to the UK Met Office climate model, and derived the 2002 annual global averaged contrail coverage and optical depth to be 0.11% and 0.2 with an estimated global mean annual contrail forcing of approximately 7.7 mW m^{-2} at the top of the atmosphere. *Chen et al.* [2012] incorporated 2006 aircraft emissions into the NCAR CESM model and compared the results with MODIS observations.

[4] In the latest IPCC AR4 report [*Forster et al.*, 2007], contrail radiative forcing is classified as one of the problems with low scientific understanding. The best estimate of 10 mW m^{-2} for persistent linear contrail radiative forcing in the year 2005 contains a large uncertainty range. The large uncertainty comes from various aspects: model deficiencies; contrail spatial distribution (coverage, optical depth, and vertical distribution); contrail size and optical properties; cloud overlap assumptions; etc. While some of the factors

[1]Department of Atmospheric Sciences, Texas A&M University, College Station, Texas, USA.
[2]Joint Institute for Earth System Science and Engineering and Department of Atmospheric and Oceanic Sciences, University of California, Los Angeles, California, USA.
[3]Science Directorate, NASA Langley Research Center, Hampton, Virginia, USA.
[4]Department of Atmospheric, Oceanic and Space Sciences, University of Michigan, Ann Arbor, Michigan, USA.

Corresponding author: P. Yang, Department of Atmospheric Sciences, Texas A&M University, College Station, TX 77843, USA. (pyang@tamu.edu)

0094-8276/12/2012GL054042

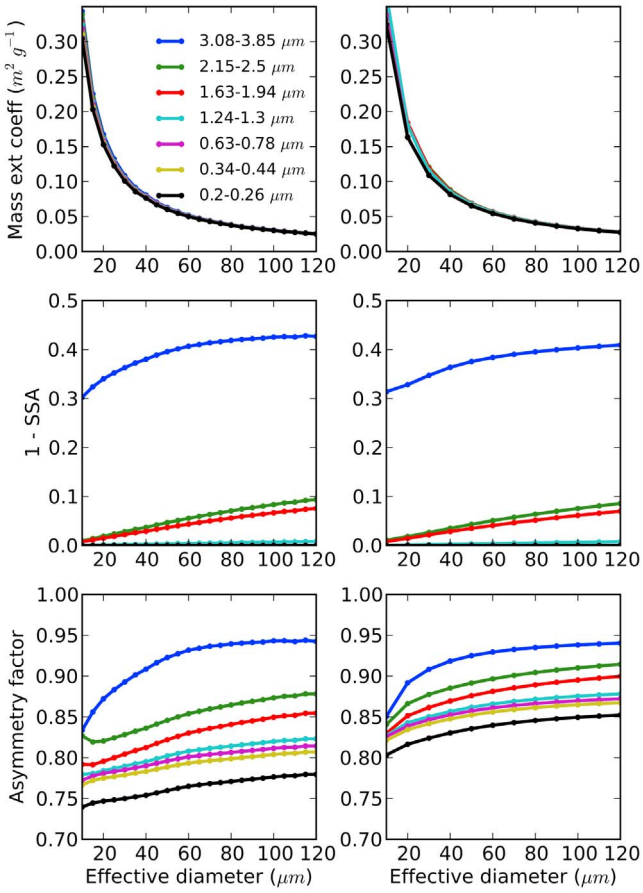

Figure 1. Example of optical property parameterizations as functions of the effective diameter for (left) natural cirrus and (right) contrail in selected spectral bands of the RRTMG radiative transfer code.

have been explored by previous studies [*Fromming et al.*, 2011; *Marquart and Mayer*, 2002; *Rap et al.*, 2010b], the uncertainties must be estimated within a comprehensive framework. This work aims to provide a consistent comparison of the potential factors influencing the forcing and to explore the largest uncertainties. The models and the simulation setup are presented in Section 2. Section 3 contains the results and discussion, and the main conclusions are summarized in Section 4.

2. Models and Simulation

[5] We employ an offline simulation approach to calculate the contrail radiative forcing. Albeit great advances have been made in online approaches, the offline approach has the advantage of easier understanding of different sensitivity studies. For the year 2006, we use the Community Atmospheric Model version 5 (CAM5) [*Neale et al.*, 2010] as the host model to provide daily atmospheric profiles and natural cloud spatial distributions in the all-sky case. The CAM5 model is driven by observed sea surface temperatures and is run at the default settings with 31 vertical levels at a $1.9° \times 2.5°$ horizontal resolution. The radiative transfer code used for the radiative flux and forcing calculation is the RRTM Model for GCMs (RRTMG) [*Iacono et al.*, 2008] for shortwave and longwave spectral bands. The RRTMG model allows for multiple choices in the various settings, such as different cloud overlap assumptions and ice cloud optical properties parameterization schemes. Furthermore, for the sensitivity tests, we implement two new parameterization schemes for natural cirrus clouds and contrails into the RRTMG. Both parameterizations are based on an ice particle scattering properties database developed by *Yang et al.* [2012]. The database contains spectrally consistent scattering, absorption, and polarization properties of atmospheric ice crystals at wavelengths from 0.2 μm to 100 μm. The natural cirrus cloud parameterization scheme uses the general ice habit mixture [*Baum et al.*, 2011], while the contrail scheme employs an ice habit mixture constrained by satellite observations [*Xie et al.*, 2012]. Figure 1 is an example of natural cirrus and contrail optical property parameterization for selected spectral bands in the RRTMG model. The optical properties, including the mass extinction coefficient, single-scattering albedo, asymmetry factor, and mass absorption coefficient, are parameterized as functions of the particle effective diameter. The natural cirrus and contrail mass extinction coefficients and single-scattering albedos are quite similar, while the largest differences are seen in the asymmetry factors. Contrails tend to have larger asymmetry factors than natural cirrus in the solar to near IR bands. Both parameterizations yield optical properties that are more sensitive to particle sizes with effective diameters smaller than $\sim$60 μm.

[6] The contrail radiative forcing strongly depends on contrail coverage and optical depth. We prescribe the same spatial distribution used by *Rap et al.* [2010b] for the 2002 annual mean global linear contrail coverage and optical depth with respective values of 0.11% and 0.2. In the control run, we assume the contrail layer is located on the 17th vertical layer (approximately 9 km in height). In the contrail optical property parameterization, an assumed particle effective diameter of 23 μm together with the random cloud layer overlap assumption is used. We design and implement model runs to examine the sensitivity of contrail forcing to various factors and assumptions. Detailed descriptions of the sensitivity tests are illustrated in Table 1. In each case, one specific factor is varied while the other factors are kept

Table 1. Description of the Sensitivity Test Cases

Case	Description
RNCO23	Using the random vertical cloud overlap assumption and contrail optical properties with a contrail effective diameter of 23 μm.
RNCO35	The same as RNCO23 case, except that a contrail effective diameter of 35 μm is used.
RNCI23	The same as RNCO23 case, except that new natural cirrus optical properties are used.
RNFU23	The same as RNCO23 case, except that the Fu parameterization scheme is used.
MRCO23	The same as RNCO23 case, except that the maximum-random vertical cloud overlap assumption is used.
RNCO23H	The same as RNCO23 case, except that the contrail layer is lifted 2 KM higher.
RNCO23OD	The same as RNCO23 case, except that 25% lower global averaged contrail optical depth is assumed.
RNCO23F	The same as RNCO23 case, except that 25% lower global averaged contrail coverage is assumed.
CRCO23	The same as RNCO23 case, except that clear-sky condition is used.

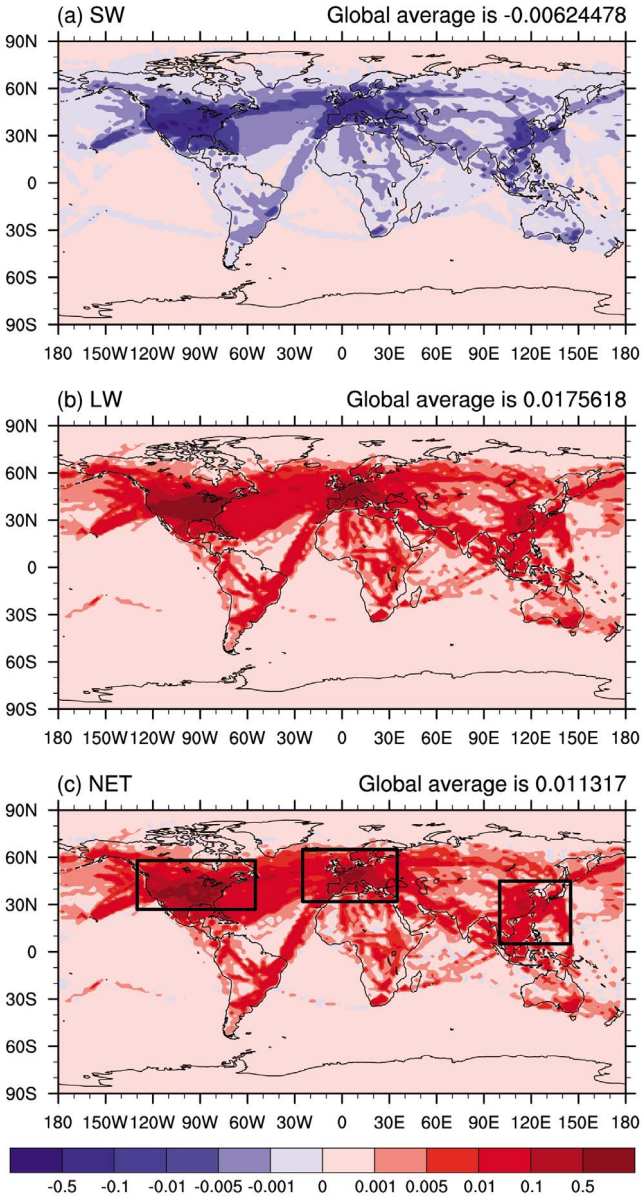

Figure 2. Simulated 2006 global annual averaged (a) shortwave, (b) longwave, and (c) net contrail radiative forcing (W m^{-2}) in the control case.

constant. In the all-sky case, natural clouds are assumed to accompany the contrail layer in the same column, with the fraction of natural clouds determined by CAM5 model simulations.

3. Results and Discussion

[7] We define contrail radiative forcing as the difference in the SW/LW/NET radiative fluxes with and without contrails at the top of the atmosphere (TOA). In the control case shown in Figure 2, the simulated 2006 global annual averaged shortwave, longwave, and net contrail radiative forcing values are −6.24 mW m^{-2}, 17.56 mW m^{-2}, and 11.32 mW m^{-2}, respectively. The net positive radiative forcing is in reasonable agreement with the best estimates from previous studies. The geographical distributions of SW, LW, and net contrail radiative forcings are most significant over continental North America, Europe, and East Asia, where the most intensive aviation activities occur. Dense inter-continental flight corridors contribute significantly to global contrail forcing. The resulting net radiative forcing generally follows the longwave distribution, which outweighs its shortwave counterpart by a factor of three. Figure 2c highlights three regional areas, and Table 2 summarizes the geographical areas and the SW, LW, and net averaged regional contrail forcing values within the three regions. The North American region is subjected to the largest averaged contrail forcing, more than ten times the global average. The regional average over Europe is slightly more than half of that over North America, whereas the East Asia region contribution is far smaller.

Table 2. Regional Contrail Radiative Forcing Over Air Traffic Intensive Areas

Region	North America	Europe	East Asia
Geographical area	27°–58° N, −130°–−55° E	32°–65° N, −25°–35° E	5°–45° N, 100°–145° E
SW forcing (m Wm^{-2})	−105.9	−40.4	−10.7
LW forcing (m Wm^{-2})	260.8	126.2	35.7
NET forcing (m Wm^{-2})	154.9	85.8	25.0

[8] The primary results from the sensitivity test cases are summarized in Table 3, where the simulated global annual mean contrail radiative forcing for each case is compared with the control case (RNCO23). The percentages in parentheses indicate relative differences between perturbation and control cases. Contrail particle size, which varies with contrail age, background meteorology, and the specific aircraft emission, is the most uncertain variable. Moreover, the contrail particle size is a difficult parameter to be retrieved on the basis of remote sensing. The RNCO35 case tests the effect on contrail radiative forcing by assuming a contrail particle to have an effective diameter 1.5 times larger than the control case. The results indicate the net forcing to increase by nearly 46% due to the combined effect of a significant decrease in shortwave forcing (−54%) and an increase in longwave forcing (10%). The results not only show the important role of contrail particle size information in the determination of contrail radiative effects, but also reveal the need for development of an accurate and reliable retrieval algorithm to determine contrail particle size by means of airborne and/or ground-based remote sensing.

[9] Two cases are selected to test sensitivity to the optical property parameterization schemes: the current natural cirrus

Table 3. Global Annual Mean Contrail Radiative Forcing for Test Cases

Case	Radiative Forcing (mW m^{-2})		
	SW	LW	NET
RNCO23	−6.24	17.56	11.32
RNCO35	−2.87 (−54.0%)	19.39 (10.4%)	16.52 (45.9%)
RNCI23	−7.52 (20.5%)	18.23 (3.8%)	10.71 (−5.4%)
RNFU23	−4.00 (−35.9%)	16.78 (−4.4%)	12.78 (12.9%)
MRCO23	−5.58 (−10.6%)	15.33 (−12.7%)	9.75 (−13.9%)
RNCO23H	−5.97 (−4.3%)	19.06 (8.5%)	13.09 (15.6%)
RNCO23OD	−2.42 (−61.2%)	13.57 (−22.7%)	11.15 (−1.5%)
RNCO23F	−2.30 (−63.1%)	13.03 (−25.8%)	10.73 (−5.2%)
CRCO23	−10.57 (69.4%)	22.72 (29.4%)	12.15 (7.3%)

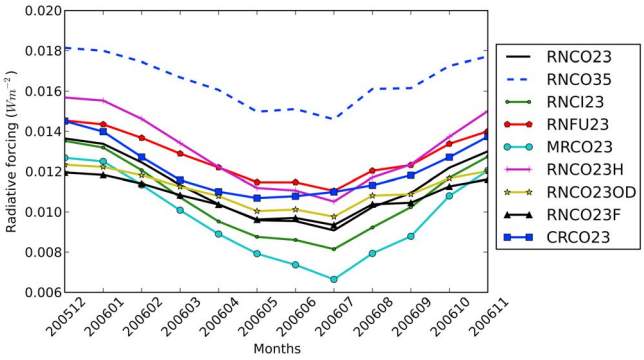

Figure 3. Monthly variation in the net contrail radiative forcing for the control case and sensitivity test cases.

parameterization (RNCI23) and the natural ice cloud parameterization developed by *Fu* [1996] (RNFU23). We find the Fu parameterization scheme, which only considers smooth hexagonal ice crystals, to significantly affect shortwave radiative forcing and to contribute a 13% increase in net forcing in comparison to the control case. The RNCI23 case yields much closer results to the control case because both the natural cirrus and contrail cloud radiative property parameterizations take into consideration a mixture of various ice crystal habits. The schemes accounting for multihabit mixtures and roughened ice particles (RNCO23 and RNCI23) should act to decrease the asymmetry factor compared with the Fu scheme case (RNFU23).

[10] *Marquart and Mayer* [2002] emphasized an important discrepancy in contrail longwave radiative forcing caused by the effective emissivity approach combined with the maximum/random cloud overlap assumption. The MRCO23 case shows that a change in the cloud overlap assumption reduces both the shortwave and longwave contrail radiative forcings by 10–12%, resulting in a 14% decrease of net forcing. The vertical position of the contrail layer is equally important. If the contrail layer is placed 2 km higher, we find the net forcing can increase to 13.09 mW m^{-2} or 15.6% larger than the control case.

[11] Contrail radiative forcing sensitivity to coverage and optical depth are tested in RNCO23OD and RNCO23F, where each parameter is reduced by 25%. The shortwave and longwave forcing components are greatly reduced in both cases, while the net forcings vary little from the control case. Compared with the RNCO23OD case, the RNCO23F case shows the effect to be stronger from contrail coverage than from optical depth. Lastly, we compare the contrail radiative forcing simulated under the clear-sky condition (CRCO23) with the all-sky condition (RNCO23). Without the masking effects of natural clouds, the shortwave and longwave radiative forcings are significantly increased. However, the net radiative forcing increases by approximately 7.3%, which is close to that reported by *Rap et al.* [2010b].

[12] Figure 3 shows the monthly variation in the net contrail radiative forcing for all the cases. We use a prescribed global contrail coverage and optical depth, which does not reflect the monthly contrail variation, and is the primary reason for the difference between the present results and those reported by *Rap et al.* [2010b]. However, the apparent monthly variation shown in Figure 3 can also be attributed to influences from other factors, for example, natural cloud masking effects. All cases show stronger contrail forcing in December and January and weaker forcing in July, except for the CRCO23 case for clear-sky contrail forcing. The RNCO35 case has the largest contrail radiative forcing, indicative of the significant effect of contrail particle effective size. The MRCO23 case is distinctive from the other cases in that it uses the maximum/random cloud overlap approximation. This case represents the largest influence from natural cloud cover, which leads to the lowest forcing and the strongest variability. The contrail height level (RNCO23H) also affects the annual variability of contrail forcing.

4. Conclusions

[13] Although great advances have been achieved in simulating global contrail radiative forcing by sophisticated GCM models, various uncertainties remain and prevent a more precise forcing determination. We employed an offline simulation approach using the CAM5 modeled atmospheric profile and cloud information as inputs and the RRTMG radiative transfer code to simulate the contrail radiative forcing. The annual mean global line-shaped contrail coverage and optical depth for the year 2002 were adapted from *Rap et al.* [2010b]. Persistent spreading contrails, i.e., contrail cirrus clouds, were not included. We used a new contrail optical properties parameterization scheme to derive the annual 2006 mean shortwave, longwave, and net contrail radiative forcings, respectively, −6.24, 17.56, and 11.32 mW m^{-2}. Regional contrail radiative forcing can be more than ten times higher than the global averages (e.g., North America).

[14] Sensitivity test cases were implemented to determine the effect of various factors on contrail radiative forcing. The results show that contrail particle effective size, contrail layer height, the model cloud overlap assumption, and contrail optical properties are among the most important factors. Thus, retrieving accurate information about the contrail particle size and vertical height are imperative to determining the correct contrail forcing. In addition to determining the contrail forcing, a more model-consistent treatment of cloud overlap and parameterizations of the contrail optical properties are vitally needed.

[15] **Acknowledgments.** This work is supported by the Aviation Climate Change Research Initiative (ACCRI) sponsored by the Federal Aviation Administration (FAA) under contracts DTRT57-10-C-10016 and DTRT57-10-X-70020. The authors thank Drs. Rangasayi Halthore and S. Daniel Jacob from the FAA for overseeing the project progress and for guidance and encouragement. The Texas A&M Supercomputing Facility (http://sc.tamu.edu) provided computing resources for conducting the research reported in this paper.

[16] The Editor thanks the two anonymous reviewers for their assistance in evaluating this paper.

References

Baum, B. A., P. Yang, A. J. Heymsfield, C. G. Schmitt, Y. Xie, A. Bansemer, Y.-X. Hu, and Z. Zhang (2011), Improvements in shortwave bulk scattering and absorption models for the remote sensing of ice clouds, *J. Appl. Meteorol. Climatol.*, *50*, 1037–1056, doi:10.1175/2010JAMC2608.1.

Burkhardt, U., and B. Karcher (2009), Process-based simulation of contrail cirrus in a global climate model, *J. Geophys. Res.*, *114*, D16201, doi:10.1029/2008JD011491.

Burkhardt, U., and B. Karcher (2011), Global radiative forcing from contrail cirrus, *Nat. Clim. Change*, *1*(1), 54–58, doi:10.1038/nclimate1068.

Chen, C. C., A. Gettelman, C. Craig, P. Minnis, and D. P. Duda (2012), Global contrail coverage simulated by CAM5 with the inventory of

2006 global aircraft emissions, *J. Adv. Model. Earth Syst.*, *4*, M04003, doi:10.1029/2011MS000105.

Forster, P., et al. (2007), Changes in atmospheric constituents and in radiative forcing, in *Climate Change 2007: The Physical Science Basis. Contribution of Working Group I to the Fourth Assessment Report of the Intergovernmental Panel on Climate Change*, edited by S. Solomon et al., pp. 131–234, Cambridge Univ. Press, Cambridge, U. K.

Fromming, C., M. Ponater, U. Burkhardt, A. Stenke, S. Pechtl, and R. Sausen (2011), Sensitivity of contrail coverage and contrail radiative forcing to selected key parameters, *Atmos. Environ.*, *45*(7), 1483–1490, doi:10.1016/j.atmosenv.2010.11.033.

Fu, Q. (1996), An accurate parameterization of the solar radiative properties of cirrus clouds for climate models, *J. Clim.*, *9*(9), 2058–2082, doi:10.1175/1520-0442(1996)009<2058:AAPOTS>2.0.CO;2.

Hong, G., P. Yang, P. Minnis, Y. X. Hu, and G. North (2008), Do contrails significantly reduce daily temperature range?, *Geophys. Res. Lett.*, *35*, L23815, doi:10.1029/2008GL036108.

Iacono, M. J., J. S. Delamere, E. J. Mlawer, M. W. Shephard, S. A. Clough, and W. D. Collins (2008), Radiative forcing by long-lived greenhouse gases: Calculations with the AER radiative transfer models, *J. Geophys. Res.*, *113*, D13103, doi:10.1029/2008JD009944.

Iwabuchi, H., P. Yang, K. N. Liou, and P. Minnis (2012), Physical and optical properties of persistent contrails: Climatology and interpretation, *J. Geophys. Res.*, *117*, D06215, doi:10.1029/2011JD017020.

Marquart, S., and B. Mayer (2002), Towards a reliable GCM estimation of contrail radiative forcing, *Geophys. Res. Lett.*, *29*(8), 1179, doi:10.1029/2001GL014075.

Meyer, R., H. Mannstein, R. Meerkotter, U. Schumann, and P. Wendling (2002), Regional radiative forcing by line-shaped contrails derived from satellite data, *J. Geophys. Res.*, *107*(D10), 4104, doi:10.1029/2001JD000426.

Minnis, P., D. F. Young, L. Nguyen, D. P. Garber, W. L. Smith Jr., and R. Palikonda (1998), Transformation of contrails into cirrus during SUCCESS, *Geophys. Res. Lett.*, *25*, 1157–1160, doi:10.1029/97GL03314.

Minnis, P., U. Schumann, D. R. Doelling, K. M. Gierens, and D. W. Fahey (1999), Global distribution of contrail radiative forcing, *Geophys. Res. Lett.*, *26*(13), 1853–1856, doi:10.1029/1999GL900358.

Minnis, P., R. Palikonda, B. J. Walter, J. K. Ayers, and H. Mannstein (2005), Contrail properties over the eastern North Pacific from AVHRR data, *Meteorol. Z.*, *14*(4), 515–523, doi:10.1127/0941-2948/2005/0056.

Neale, R. B., et al. (2010), Description of the NCAR Community Atmosphere Model (CAM 5.0), *NCAR Tech. Note NCAR/TN-486+STR*, Natl. Cent. for Atmos. Res, Boulder, Colo.

Penner, J. E., D. H. Lister, D. J. Griggs, D. J. Dokken, and M. McFarland (Eds.) (1999), *Aviation and the Global Atmosphere*, 373 pp., Cambridge Univ. Press, Cambridge, U. K.

Ponater, M., S. Marquart, and R. Sausen (2002), Contrails in a comprehensive global climate model: Parameterization and radiative forcing results, *J. Geophys. Res.*, *107*(D13), 4164, doi:10.1029/2001JD000429.

Rap, A., P. M. Forster, J. M. Haywood, A. Jones, and O. Boucher (2010a), Estimating the climate impact of linear contrails using the UK Met Office climate model, *Geophys. Res. Lett.*, *37*, L20703, doi:10.1029/2010GL045161.

Rap, A., P. M. Forster, A. Jones, O. Boucher, J. M. Haywood, N. Bellouin, and R. R. De Leon (2010b), Parameterization of contrails in the UK Met Office Climate Model, *J. Geophys. Res.*, *115*, D10205, doi:10.1029/2009JD012443.

Sausen, R., et al. (2005), Aviation radiative forcing in 2000: An update on IPCC (1999), *Meteorol. Z.*, *14*(4), 555–561, doi:10.1127/0941-2948/2005/0049.

Travis, D. J., A. M. Carleton, and R. G. Lauritsen (2002), Climatology: Contrails reduce daily temperature range—A brief interval when the skies were clear of jets unmasked an effect on climate, *Nature*, *418*(6898), 601, doi:10.1038/418601a.

Xie, Y., P. Yang, K.-N. Liou, P. Minnis, and D. P. Duda (2012), Parameterization of contrail radiative properties for climate studies, *Geophys. Res. Lett.*, doi:10.1029/2012GL054043, in press.

Yang, P., L. Bi, B. A. Baum, K. N. Liou, G. W. Kattawar, M. I. Mishchenko, and B. Cole (2012), Spectrally consistent scattering, absorption, and polarization properties of atmospheric ice crystals at wavelengths from 0.2 μm to 100 μm, *J. Atmos. Sci.*, doi:10.1175/JAS-D-12-039.1, in press.